A study of mesoscale gravity waves over the North Atlantic with satellite observations and a mesoscale model

Dong L. Wu
Jet Propulsion Laboratory, California Institute of Technology, Pasadena, California, USA

Fuqing Zhang
Department of Atmospheric Sciences, Texas A&M University, College Station, Texas, USA

Received 3 June 2004; revised 4 August 2004; accepted 19 August 2004; published 25 November 2004.

[1] Satellite microwave data are used to study gravity wave properties and variabilities over the northeastern United States and the North Atlantic in the December–January periods. The gravity waves in this region, found in many winters, can reach the stratopause with growing amplitude. The Advanced Microwave Sounding Unit-A (AMSU-A) observations show that the wave occurrences are correlated well with the intensity and location of the tropospheric baroclinic jet front systems. To further investigate the cause(s) and properties of the North Atlantic gravity waves, we focus on a series of wave events during 19–21 January 2003 and compare AMSU-A observations to simulations from a mesoscale model (MM5). The simulated gravity waves compare qualitatively well with the satellite observations in terms of wave structures, timing, and overall morphology. Excitation mechanisms of these large-amplitude waves in the troposphere are complex and subject to further investigations. *INDEX TERMS:* 3334 Meteorology and Atmospheric Dynamics: Middle atmosphere dynamics (0341, 0342); 3329 Meteorology and Atmospheric Dynamics: Mesoscale meteorology; 3362 Meteorology and Atmospheric Dynamics: Stratosphere/troposphere interactions; 3394 Meteorology and Atmospheric Dynamics: Instruments and techniques; 3384 Meteorology and Atmospheric Dynamics: Waves and tides; *KEYWORDS:* mesoscale gravity waves, North Atlantic, satellite observations

Citation: Wu, D. L., and F. Zhang (2004), A study of mesoscale gravity waves over the North Atlantic with satellite observations and a mesoscale model, *J. Geophys. Res.*, *109*, D22104, doi:10.1029/2004JD005090.

1. Introduction

[2] Gravity waves (GWs) play important roles in determining atmospheric circulations and thermal structures. Since many of these waves are not resolved in global climate and weather prediction models, the momentum and energy releases from wave breaking must be incorporated through subgrid-scale parameterizations [e.g., *Hamilton*, 1996; *McLandress*, 1998; *Kim et al.*, 2003]. In addition, GW processes have direct impacts on mesoscale precipitation bands through coupling to convection and cloud dynamics [*Bosart et al.*, 1999]. The GW role on polar stratospheric cloud formation, which has been recognized as being important to ozone chemistry [*Leutbecher and Volkert*, 2000; *Dörnbrack et al.*, 2002], remains to be quantified.

[3] GW excitations are mostly related to processes of convection, jet stream, and flow over topography in the lower atmosphere [*Fritts and Alexander*, 2003, and references therein]. However, knowledge of wave source distributions and properties remains poor, which is a major uncertainty in GW parameterizations. Currently, GW drag parameterizations in global circulation models are semiarbitrary and lacking observational guidance on wave source properties and excitation conditions [e.g., *McFarlane*, 1987; *Chun and Baik*, 2002]. More quantitative and comprehensive understandings on wave generation and propagation are needed, and these processes should be studied jointly under realistic atmospheric conditions from the troposphere up to the stratosphere and mesosphere.

[4] Mesoscale models (e.g., Pennsylvania State University (PSU)/University Corporation for Atmospheric Research mesoscale model MM5) on a domain as large as a hemisphere can simulate realistic GWs in the troposphere and stratosphere and have been the primary tool for investigating wave generation and propagation properties [e.g., *Zhang and Fritsch*, 1988; *Schmidt and Cotton*, 1990; *Zhang*, 2004]. Mesoscale models can reveal detailed wave structures, energy sources, and maintenance mechanisms that are difficult to measure from space [*Zhang and Koch*, 2000; *Koch et al.*, 2001; *Zhang et al.*, 2001, 2003; *Lane et al.*, 2004]. Some specialized wave models (e.g., Mountain Wave Forecast Model) have also been used to study wave propagation properties from the source region to as high as the thermosphere [*Eckermann and Preusse*, 1999].

[5] Modeled GW properties or effects require observational verifications, which are often difficult to obtain. Assimilated or analysis/reanalysis data sets are not independent observations because of potential biases from the underlining models. Mesoscale phenomena in these data sets depend largely on the rejection criteria used. Conventional observations (e.g., radiosondes) provide few reports

0148-0227/04/2004JD005090

over oceans and lack the mapping ability. Because of limited height coverage of the ground-based measurements the fate of large-amplitude GW events and their impacts on the upper air dynamics were little explored. Furthermore, substantial uncertainties exist in the commonly used hodograph method to retrieve GW characteristics from the sounding profiles [*Zhang et al.*, 2004].

[6] Satellite observations now provide a valuable source for GW studies in the middle and upper atmosphere, especially over oceans and other radiosonde-sparse regions. Recent advances in space technology offer appreciable resolution and precision for mesoscale GW observations on a global basis. Among these successful applications, passive microwave sounders have been utilized to map GW activity in the stratosphere, e.g., Microwave Limb Sounder (MLS) [*Wu and Waters*, 1996; *McLandress et al.*, 2000; *Jiang et al.*, 2004] and Advanced Microwave Sounding Unit-A (AMSU-A) down to the tropopause [*Wu*, 2004]. These studies analyzed raw radiance measurements, rather than retrieved temperature, to preserve as much small-scale information as possible. The radiance variances inferred in these analyses are interpreted as temperature perturbations due to GWs. This claim is supported by the analysis method used where only wave components of short horizontal wavelengths ($<\sim$100 km for MLS or $<\sim$600 km for AMSU-A) are retained [*Wu and Waters*, 1996; *Wu*, 2004]. Because small-scale wave features are often transient and weak in amplitude and most satellite instruments are not designed to measure such weak features, it is important not to introduce additional error in the data analyses (e.g., by retrieving atmospheric temperature). Additional data manipulations are often destructive to small-scale wave signatures or make the results complicated to interpret.

[7] The strong GW enhancement over the North Atlantic (NA) region has been previously observed by MLS, but the wave excitation mechanism(s) and propagation properties were unclear because of MLS height and sampling limitations [*McLandress et al.*, 2000]. To explore mesoscale waves at lower altitudes, we choose to analyze AMSU-A radiances for the December–February periods when GWs are active over the NA, in particular, during a strong GW event on 19–21 January 2003. This observational study and follow-on modeling investigations are aimed to improve our understanding of GW sources and impacts on the tropospheric and middle atmospheric dynamics.

[8] This paper is organized to first describe mean observed characteristics and interannual variations of the NA GWs in the December–January period (section 2), followed by a detailed analysis of the wave properties observed on 19–21 January 2003 when an upper level trough swept through the east coast of the United States (section 3). Large-amplitude GWs excited during this period appear to have multiple components associated with jet streak, orographic forcing, and convective activity in the troposphere. An MM5 simulation of the 19–21 January 2003 event is run to compare with the AMSU-A observations in the upper troposphere and lower stratosphere. Wave generation mechanisms and the roles of a strong upper tropospheric jet streak are discussed in section 4.

2. MLS and AMSU-A GW Observations

[9] The 63-GHz O_2 radiances measured by MLS on the Upper Atmosphere Research Satellite are sensitive to temperature perturbations of short (<100 km) horizontal and long (>10 km) vertical wavelengths [*Wu and Waters*, 1996]. These radiance perturbations can be interpreted as atmospheric gravity wave motions and can be used to map GW activity in the stratosphere and mesosphere [*McLandress et al.*, 2000; *Jiang et al.*, 2004]. Much of the MLS GW variances in the Northern Hemisphere (NH) winter were thought to be of orographic origin [*Jiang et al.*, 2004], and overall good agreement was found over elevated terrain in comparison with the Naval Research Laboratory Mountain Wave Forecast Model. For example, during December 1991 to January 1992 the MLS GW variance maps show clear enhancements over mountains in Alaska, Canada, Greenland, Scandinavia, and Russia (Figure 1).

[10] However, GWs over oceans (e.g., the NA region) have not been investigated in detail, and the linkage between the troposphere and the stratosphere is not yet clear. In the stratosphere, as observed by MLS, the enhanced GW activity extends from Canada to south of Greenland in the 1991–1992 winter (Figure 1), and the NA component becomes increasingly important as waves propagate to higher altitudes. The overall GW distribution patterns are similar among the MLS maps at 33–48 km with slight variance differences. At 61 km the NA component makes up $\sim$20% of the total wave variance between 30° and 70°N latitudes.

[11] For GWs in the upper troposphere and lower stratosphere, *Wu* [2004] extended the MLS analysis method to AMSU-A radiance data that have better horizontal resolution and longer records. The AMSU-A radiances are sensitive to mesoscale GWs of long (>10 km) vertical wavelengths, and their coverage is excellent with almost no gaps between orbits. The AMSU-A instrument has a total of 15 sounding channels, six of which (channels 9–14) have the peak of temperature weighting function above 18 km (i.e., $\sim$18, $\sim$21, $\sim$26, $\sim$33, $\sim$38, and $\sim$45 km). Because our GW analyses use the AMSU-A radiances directly, the wave amplitude and variance are associated uniquely with each channel (or the altitude featured). Thus the vertical resolution of the radiance variance, instead determined by the number of sounding channels used, is limited by the thickness of temperature weighting function. Caution is required to use AMSU-A channels 1–8 and 15 since surface emission and cloud scattering may affect these radiances and their variances. GWs are normally detectable if wave amplitudes are greater than the instrument noise (varying between 0.15 K for channel 9 and 0.8 K for channel 14), but the detection threshold can go below

Figure 1. GW variance maps from UARS MLS descending orbits for December 1991 to January 1992 at (a) 38, (b) 48, and (c) 61 km. Variances are averaged to 4° × 5° latitude-longitude grid boxes. Region over the northwestern Atlantic, enclosed by the circle, is of interest in this study where GWs are frequently generated and propagate into the stratosphere and mesosphere.

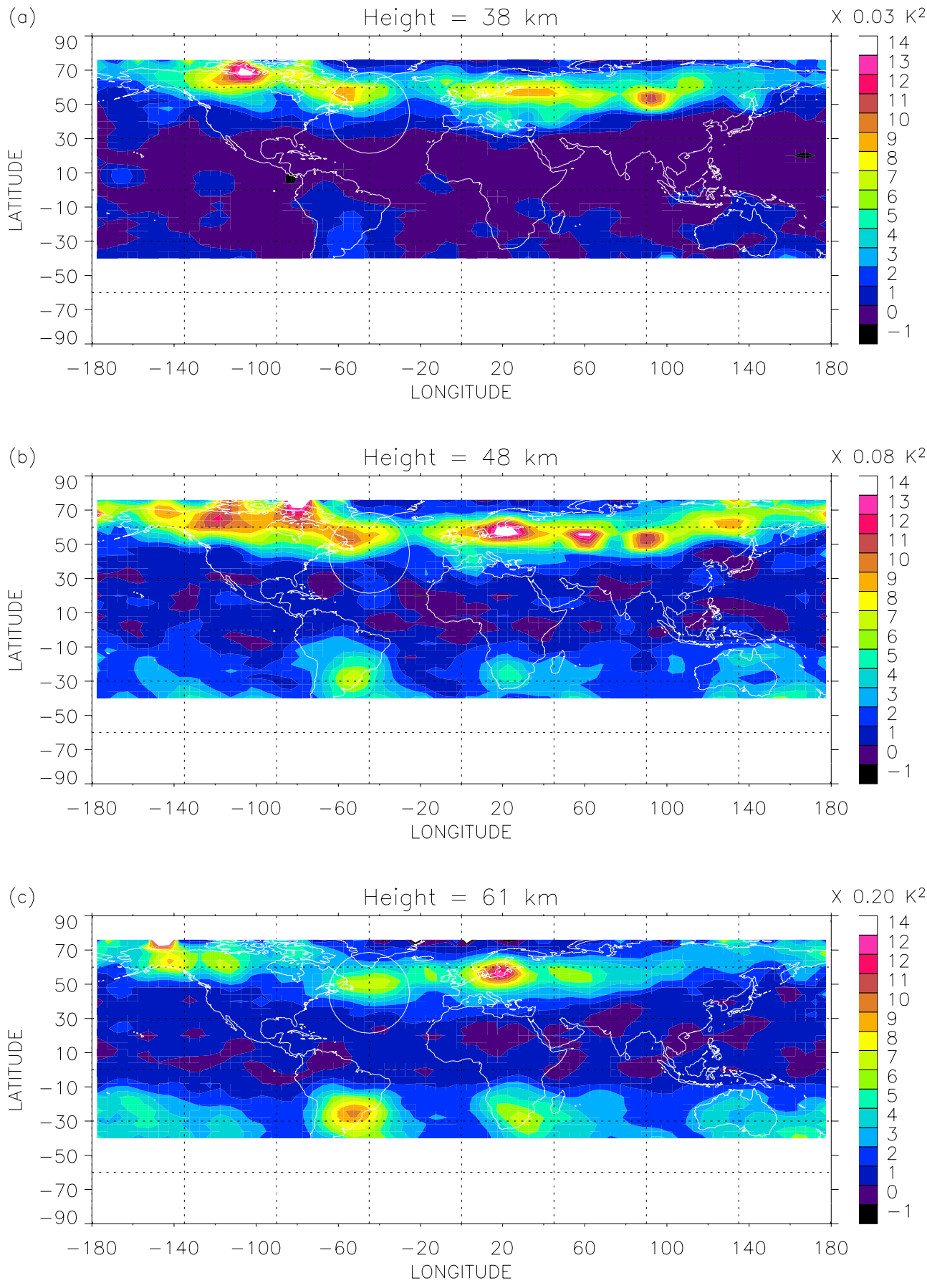
(a)
Height = 38 km
X 0.03 K²
(b)
Height = 48 km
X 0.08 K²
(c)
Height = 61 km
X 0.20 K²
LATITUDE
LONGITUDE
90
70
50
30
10
−10
−30
−50
−70
−90
−180
−140
−100
−60
−20
20
60
100
140
180
14
13
12
11
10
9
8
7
6
5
4
3
2
1
0
−1

Figure 1

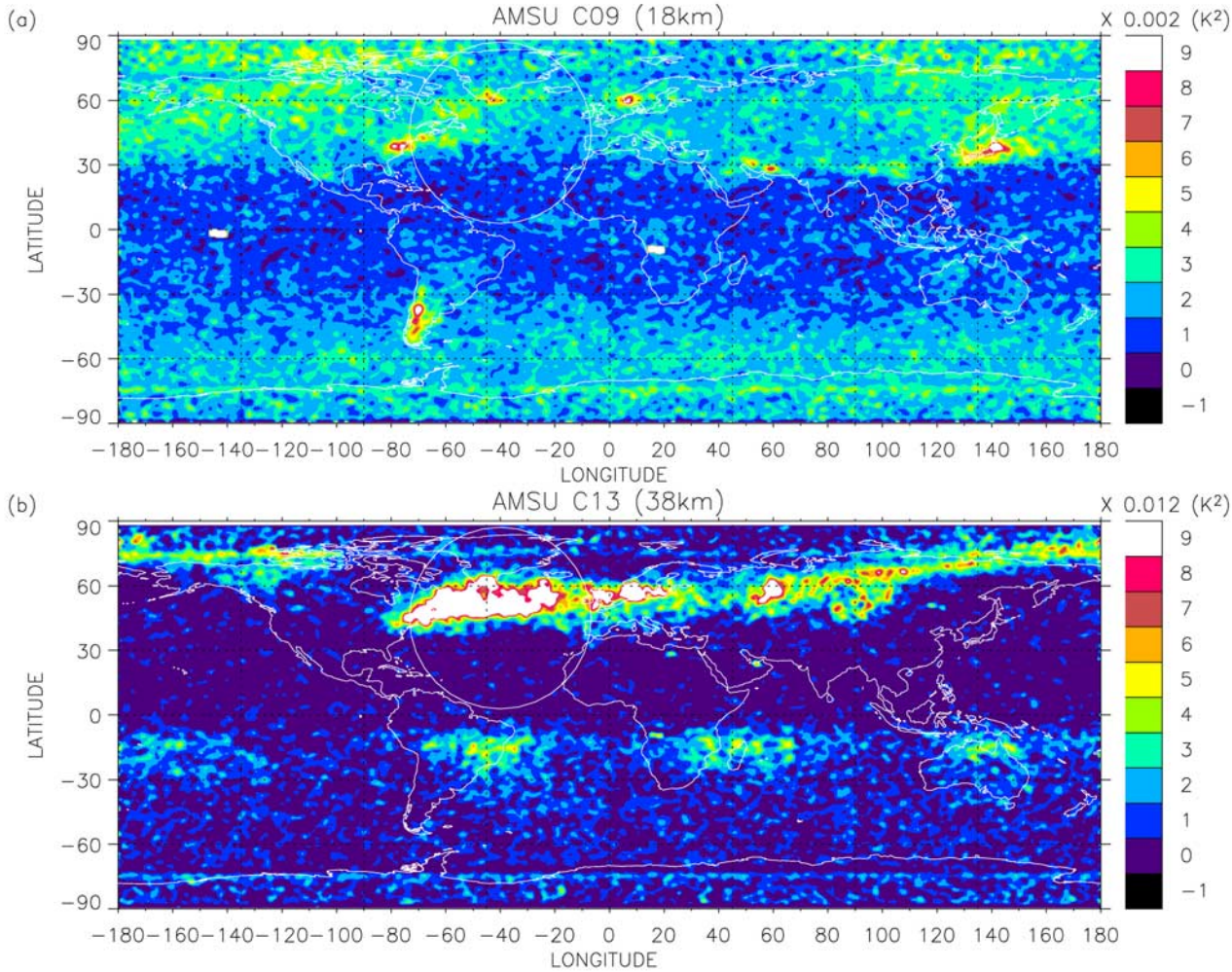

Figure 2. AMSU-A GW variance maps for December 2002 to January 2003 at (a) 80 hPa (∼18 km) and (b) 5 hPa (∼38 km). Variances are averaged to 0.5° × 0.5° latitude-longitude grid boxes. Bad measurements are indicated by the white areas.

the noise floor with the careful variance analyses [*Wu and Waters*, 1996; *Wu*, 2004]. Despite the improved coverage, AMSU-A measurements still temporally under sample the mesoscale GWs with periods of 1–6 hours and phase speeds of 10–40 m s^{-1}. Thus for wave properties we rely mostly on the AMSU-A three-dimensional (3-D) snapshots to deduce wave structures.

[12] Shown in Figure 2 are AMSU-A GW variance maps at 80 hPa (∼18 km) and 5 hPa (38 km) as observed by NOAA 15, NOAA 16, and NOAA 17 satellites during December 2002 to January 2003. These AMSU-A variances are obtained from radiance fluctuations sampled at 32°–48° viewing angles (with respect to nadir), compared quite differently to the limb case (∼66° from nadir) for MLS. The viewing angle is important for radiance sensitivity to GW-induced temperature perturbations as a result of the convolution between 3-D wave structures and instrument weighting functions associated with these satellite observations. Large viewing angles with respect to nadir increase the radiance sensitivity to the orientation of wave propagation. The wave variances are likely to be greater for the cases when wave fronts are in line with the instrument line of sight (LOS) and smaller when wave fronts propagate across the LOS.

[13] The climatology of the 38-km AMSU-A variance shows a similar distribution of GW activity to the MLS result for the 1991–1992 winter, where the AMSU-A variances over the NA are more dominating than ones in the MLS maps. In the 18-km map, orographic sources stand out as wave activity enhances near elevated terrains, including the southern Andes, New Zealand, the Appalachians, southern Greenland, Scandinavia, Urals, Putoran, Zagros, Himalayas, and Japan. Most of these mountain waves did not propagate above 38 km, except maybe over Scandinavia, the Urals, and Putoran. The enhanced GW activity as observed by AMSU-A at 38 km is consistent with the MLS results. In addition to orographic components, there are weak but significant enhancements in the Southern Hemisphere subtropics from deep convection, which appear both in the MLS maps and in the AMSU-A maps. These convectively generated GWs have been investigated previously with MLS data [*McLandress et al.*, 2000; *Jiang et al.*, 2004]. Compared to MLS, it is more difficult for the AMSU-A instrument to detect convectively generated

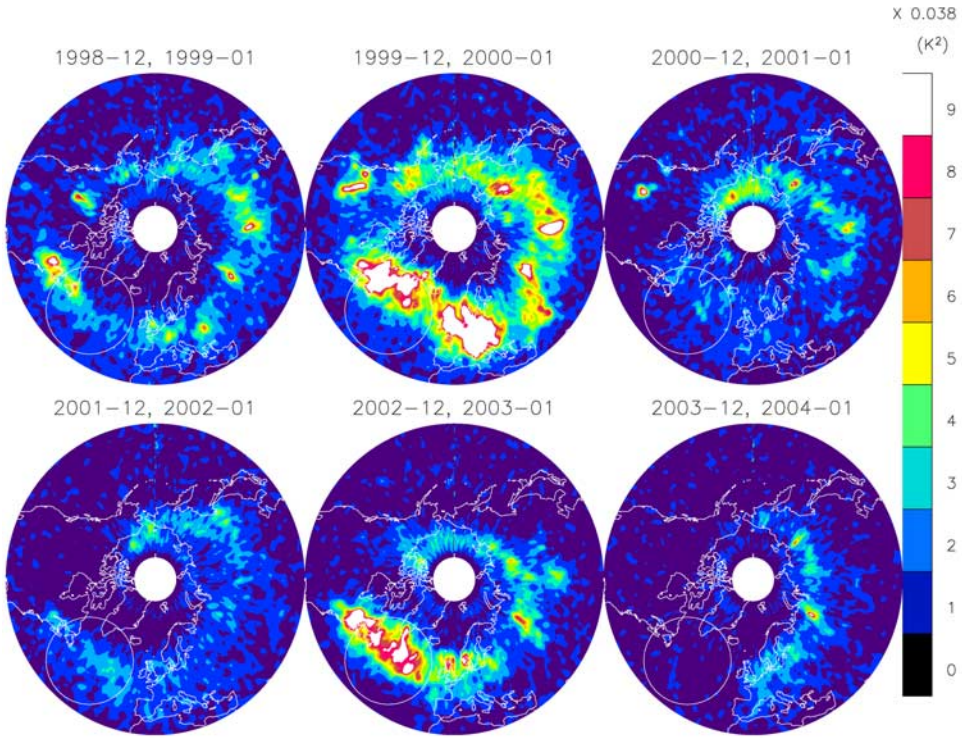

Figure 3. Interannual variations of GW activity from AMSU-A for 1998–2004 North Atlantic winters (December–January). Different from the maps in Figure 2, the AMSU-A data are solely from NOAA 15 so that the instrument noise in these maps is consistent. Grid box sizes are the same as in the AMSU-A maps in Figure 2.

GWs because of more instrument noise and larger field of view (FOV) averaging.

[14] The MLS and AMSU-A observations also exhibit important differences, mostly due to the different time periods when these observations were made. In fact, there is strong interannual variability in the stratospheric GW activity over the NH as revealed by AMSU-A. Because the tropospheric and stratospheric jet streams can strongly affect wave generation and propagation, significant correlation is expected between GW enhancement and these jet streams. As shown in Figure 3, the NOAA 15 AMSU-A GW variance data indicate that the wave activity in 1999–2000 and 2002–2003 winters was stronger than wave activity in other years. For the 2002–2003 winter events studied in this paper, the wave NA activity dominates the total wave variance. It is interesting to note that the NA activity is almost absent at 5 hPa in the 2003–2004 winter. Also, in the 6-year AMSU-A observations, no significant wave enhancement is observed from North Pacific winter storms, in which the intensity is generally weaker than that of Atlantic winter storms [*Hoskins and Hodges*, 2002].

[15] Despite differences in viewing geometry and observing period the MLS and AMSU-A maps both exhibit persistent wave activity over the NA during the December–January period. These observations raise important questions about origins of the waves in the troposphere and their impacts on upper atmospheric dynamics. What are the excitation mechanisms of these mesoscale GWs, how frequent are these excitations, and how many reach or break in the stratosphere and above? What is the role of the NA GWs in the observed patterns of climatological anomalies in the stratosphere (e.g., Arctic oscillations)? Motivated by these questions, we conducted a detailed investigation utilizing AMSU-A observations and MM5 simulations on GW events during 19–21 January 2003.

3. The 19–21 January 2003 Event

[16] In the troposphere, large-amplitude wave events are infrequent but may be persistent and maintained for a relatively long (1–3 days) period of time [*Ramamurthy et al.*, 2001; *Koppel et al.*, 2000]. These waves typically have wavelengths of 50–500 km, periods of 0.5–4 hours, surface amplitudes of 0.5–15 hPa, and phase velocities of 15–35 m s^{-1} and are capable of organizing precipitation into bands, creating damaging winds, sleet, and blizzard conditions, and triggering instabilities that lead to the development of severe convection downstream. The situation becomes more complex when sensible heating over elevated terrain is involved. According to the survey compiled by *Uccellini and Koch* [1987], these large-amplitude waves tend to appear in the vicinity of jet streaks and within the cool side of a surface warm or stationary front.

3.1. Meteorological Conditions

[17] During 18–20 January 2003 a long-wave, fast traveling upper trough moved into the eastern United States (Figure 4). A strong jet with speed >70 m s^{-1} was developed at 300 hPa, setting up favorable conditions for the jet streak GW genesis in the upper troposphere. The

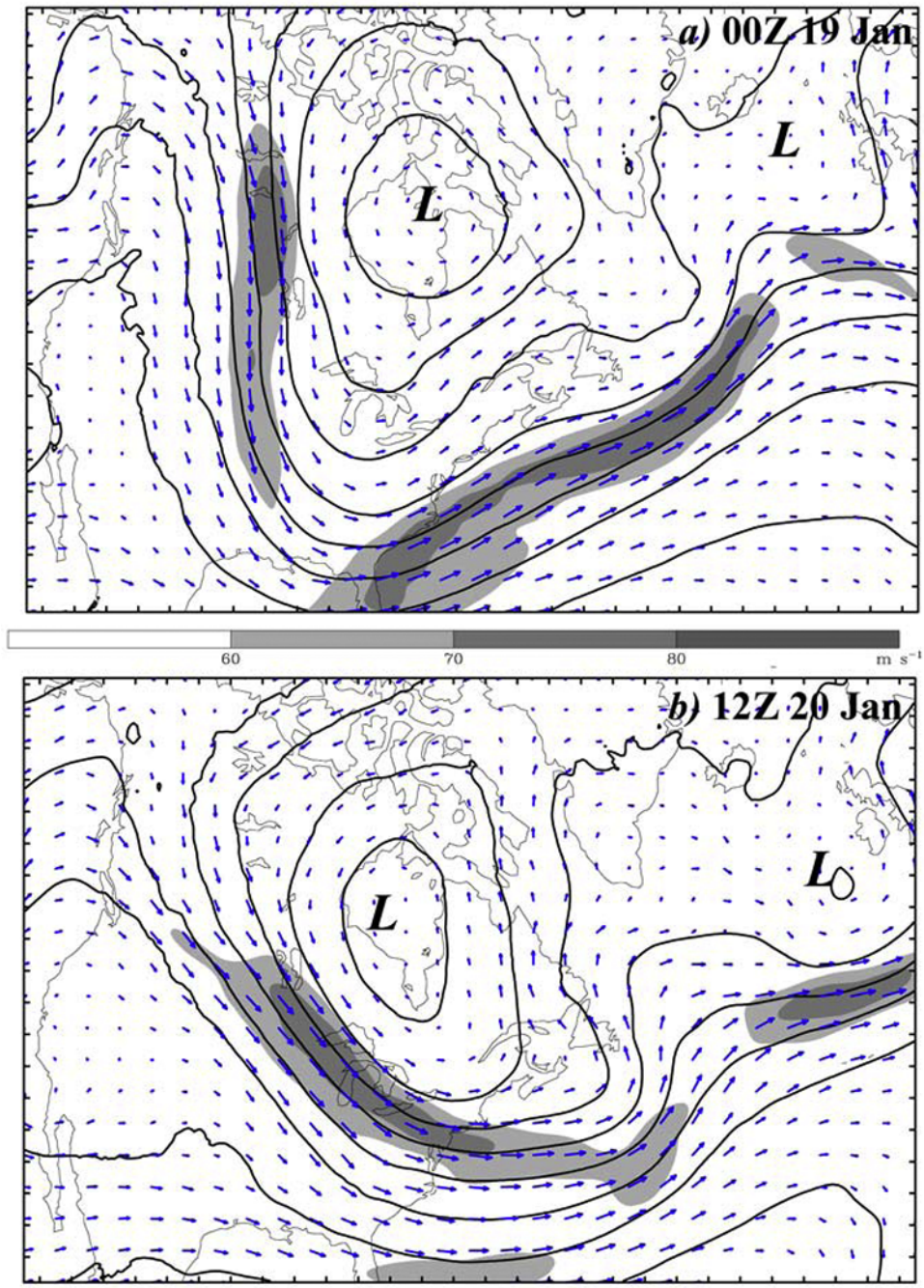

Figure 4. European Centre for Medium-Range Weather Forecasts 300-hPa geopotential heights (every 20 decameters (dam)) and horizontal winds (in vectors, speed >60 m s^{-1} where shaded) at (a) 0000 UT on 19 January and (b) 1200 UT on 20 January 2003. At 1200 UT on 20 January 2003 the trough moved to the eastern United States, creating strong winds toward the Appalachians. Low-pressure centers are indicated by letter "L."

cyclonic exit region of the upper jet streak is interesting to watch in launching mesoscale gravity waves [*Uccellini and Koch*, 1987; *Zhang*, 2004]. This synoptic-scale feature affected a large area of North America, and heavy snowfalls on the east coast were reported. Moving eastward, the trough on 20 January 2003 caused a strong cross-Appalachian wind flow, setting up a perfect condition for launching mountain waves.

[18] A similar strong cyclone-related GW event on 4 January 1994 was documented by *Bosart et al.* [1999] when heavy snowfall was reported along the Appalachians on the west side of wave fronts. The phase speed of these GWs was reported around 35–40 m s^{-1} with complex mesoscale structures imbedded in the cyclone environment. Using mesoscale model simulations with MM5, *Zhang et al.* [2001] proposed a complex sequence of geostrophic

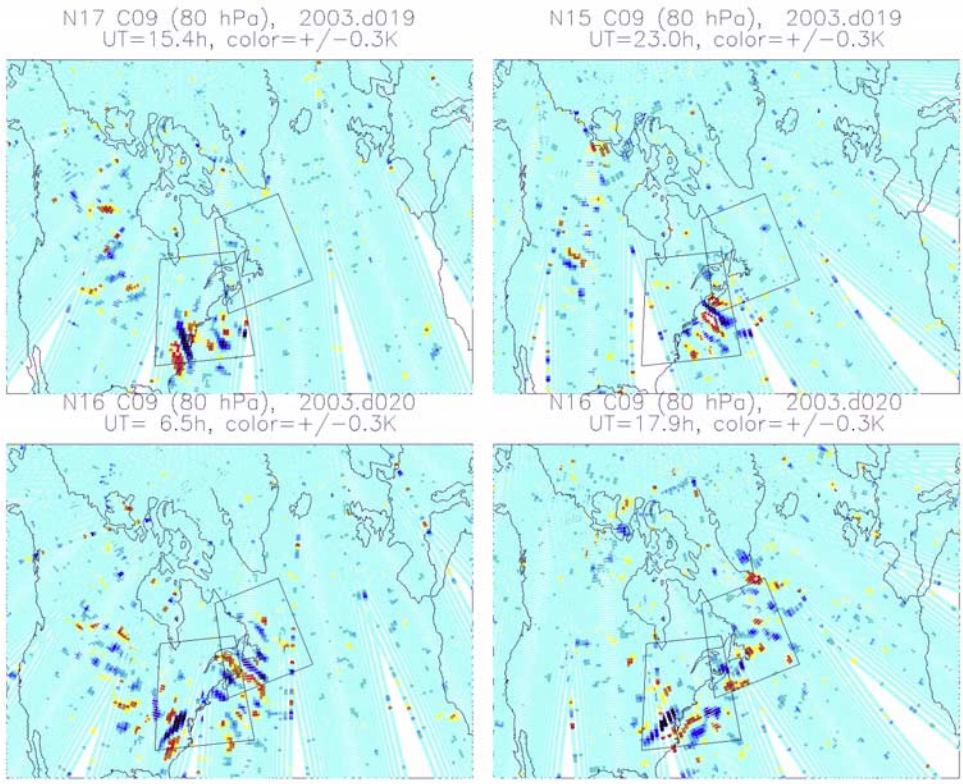

Figure 5. AMSU channel 9 (∼80 hPa) radiance perturbation maps at four crossing times during 19–20 January 2003. Crossing time is defined by the orbit crossing the map center. Adjacent orbits are separated by ∼100 min in time. Two regions, indicated by the boxes, are of special interest in this study. Region 1 (right) is used to study GWs propagating off North America, whereas region 2 (left) is used to monitor orographic waves from the Appalachians.

adjustment processes associated with the upper tropospheric jet streak, which were responsible for initiating the gravity waves.

3.2. AMSU-A Radiance Perturbation Maps

[19] Four similar AMSU-A instruments are currently in operation: three on National Oceanic and Atmospheric Administration (NOAA) satellites NOAA 15 (since May 1998), NOAA 16 (since September 2000), and NOAA 17 (since June 2002), and one on NASA Aqua satellite (since May 2002), with the ascending equator-crossing time at 1930, 1400, 2200, and 1330 UT, respectively. As a result the NA region is sampled every ∼4 hours jointly by these instruments. The NOAA AMSU-A has a scan swath of ∼2300 km cross track, and each FOV produces a footprint size of ∼50 km at nadir and ∼110 km for the outermost beam with a scan angle of 48.3° from nadir. The spacing between the adjacent FOVs matches the FOV size so that a scan covers the whole swath without gaps.

[20] To extract GW signals from the AMSU-A radiance measurements during a single orbit, the background radiance along the orbit needs to be determined first. It is important not to use radiative transfer models or other planetary wave filtering methods to estimate this background because the real atmosphere is unknown and the (radiative transfer or planetary wave) models could misrepresent the background field. Instead, we choose an empirical method for the background calculation, which uses a 2-D running mean on the raw radiance data. For this study, a 2-D nine-point running window is used for the background estimation, which treats any variations with scales >∼600 km as the 2-D background. Hence the difference between the measured and smoothed radiances (or the background) yields wave components with scales <∼600 km. Since the cross-track AMSU-A has a finite number of measurements (30), the 2-D smoothing method has a problem at the swath edge (four FOVs on each side) where it is replaced by the nine-point 1-D smoothing (along track). The smoothing method used here will remove most of the instrument systematic error, including the so-called ''limb'' or ''cross-track-asymmetry'' effect associated with AMSU-A observations [*Goldberg et al.*, 2001] and the FOV-to-FOV biases (at 0.1- to 0.2-K levels) as reported by *Wu* [2004].

[21] Figure 5 presents four radiance perturbations maps from AMSU-A channel 9 (∼80 hPa) during 19–20 January 2003. Two episodes of enhanced gravity activity are observed at this level during this period of interest. The first episode started on 19 January offshore of the east coast with wave fronts lined up in the southeast-northwest direction. It propagates away from the continent at a phase speed of ∼15 m s^{-1}, which can be estimated from consecutive orbits (∼1.5-hour difference) of the same satellite or adjacent orbits from different satellites. The second wave episode occurred on 20 January near the Appalachians with wave fronts along the mountain ridge. These waves were

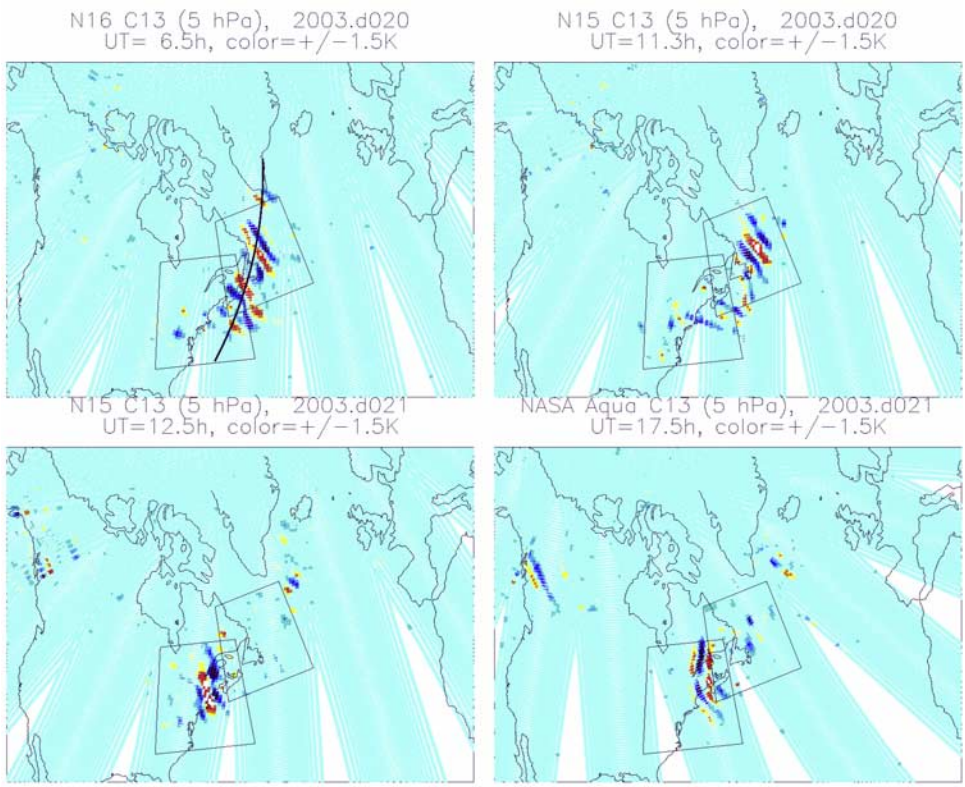

Figure 6. AMSU-A channel 13 (∼5 hPa) radiance perturbation maps at four crossing times during 20–21 January 2003. Crossing time and the two regions of interest are defined in the same way as in Figure 4. Thick line indicates where the cross section for Figure 8 is cut.

further enhanced on late 20 and early 21 January 2003 over North Carolina and Georgia of the United States. Other wave activities are also evident during this period, including several features near the Rockies and in Canada, but the amplitudes of these waves are somewhat weaker.

[22] Aloft, AMSU-A channel 13 (∼5 hPa) radiances show amplified but delayed perturbations (Figure 6) after the wave appeared at 80 hPa. Wave characteristics have changed somewhat at this altitude, compared to the events observed by channel 9. Waves from the first episode exhibit similar wavelength, phase speed, and propagation direction but last slightly longer. The first episode reaches the southern tip of Greenland before its breakdown in that neighborhood. Waves associated with the Appalachians propagate vertically but remain in the vicinity of their source region, exhibiting different (south-north) wave phase lines at 5 hPa (versus 80 hPa) and a wake-like feature at 1730 UT.

3.3. Wave Structures and Propagation

[23] Figure 7 shows a close view of a snapshot of the NA waves (i.e., the first episode) at 0630 UT on 20 January 2003 from six pressure levels. The estimated horizontal wavelengths range between 300 and 600 km, dominated by a 500-km component. At 5 hPa, waves of large amplitude spread to a wider area than those at 80 hPa, but the location of the maximum amplitudes at 5 hPa corresponds well to the maxima at 80 hPa in general.

[24] Figure 8 is the vertical cross section of wave amplitudes from radiance perturbations in channels 7–14, showing phase lines tilted upstream. These waves appear to have long (20–30 km) vertical wavelengths (λz), which represent a very different class of mesoscale GWs from those $\lambda z = 2$–5 km waves studied elsewhere [e.g., *Uccellini and Koch*, 1987] in the low and middle troposphere. These long-λz GWs are ideal for instruments like AMSU-A to measure which has temperature weighting functions of thickness >10 km.

[25] We use all the AMSU-A data from NOAA 15, NOAA 16, NOAA 17, and NASA Aqua satellites to monitor propagation of the first wave episode at 5 hPa. The wave track is shown in Figure 9. We start tracking this wave episode at 0536 UT on 20 January after it was initiated near Newfoundland around 1600 UT on 19 January. This wave episode persists for nearly 2 days with a coherent phase speed between 80 and 5 hPa during its propagation. During the fast traveling period (1100–1600 UT on 20 January) it posted a group velocity of ∼40 m s^{-1}, which is somewhat greater than the phase speed estimated in section 3.2 from channel 9 observations.

3.4. Time Series

[26] Mesoscale GWs generated in the troposphere have profound implications for the dynamics in the stratosphere and mesosphere. Their roles in sudden stratospheric warming and northern annular mode generation remain puzzling. To study the connection between GWs in the stratosphere and ones excited in the upper troposphere, we identify two regions, highlighted in Figures 5–6, and monitor the time series of wave amplitudes during the month of January

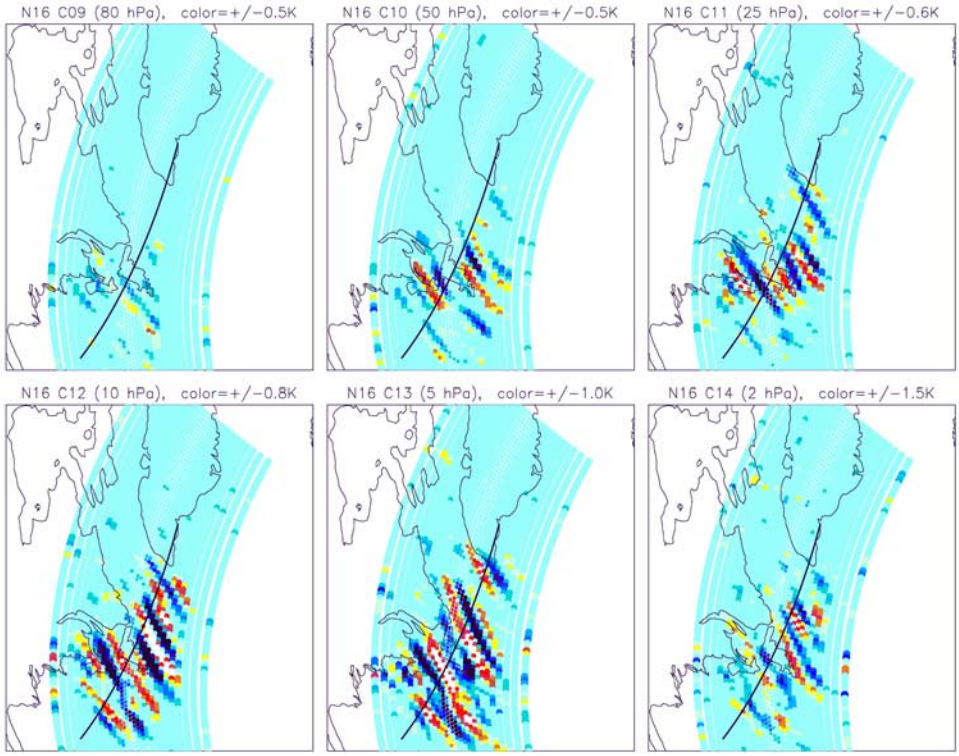

Figure 7. Radiance perturbations from NOAA 16 AMSU-A channels 9–14 at 0630 UT on 20 January. Peak-to-peak color is indicated above each image.

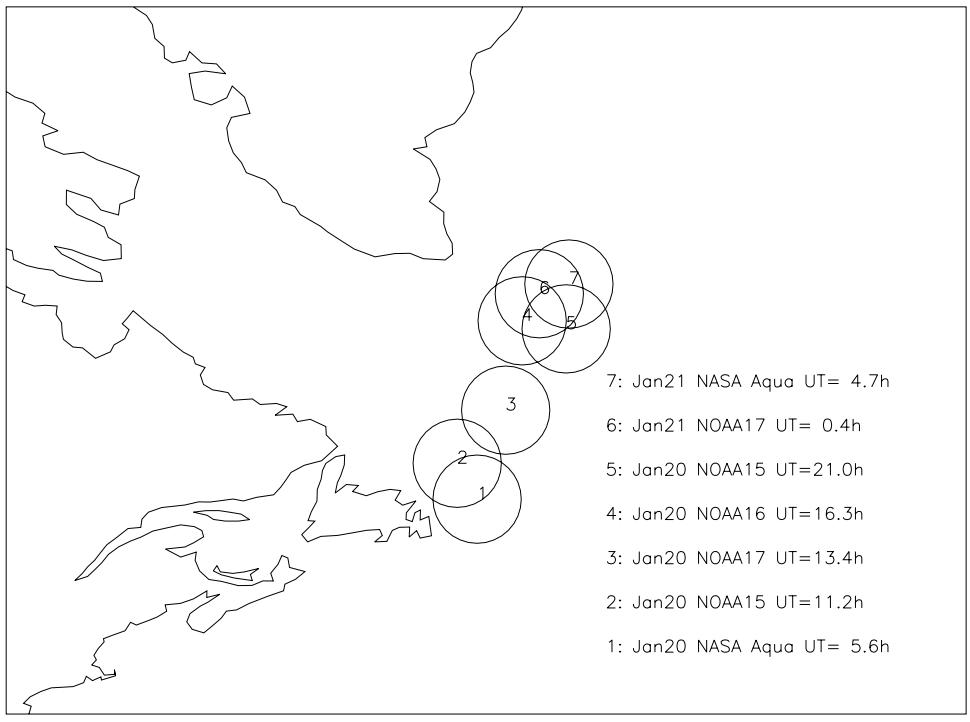

Figure 8. Vertical cross section of wave structures as observed from AMSU-A channels 7–14 at ~0600 UT on 20 January. Cross section is cut through the track indicated by the thick line in Figure 6. Latitude-height plot clearly shows that waves are tilted upstream, as expected for the jet streaks generated from instability.

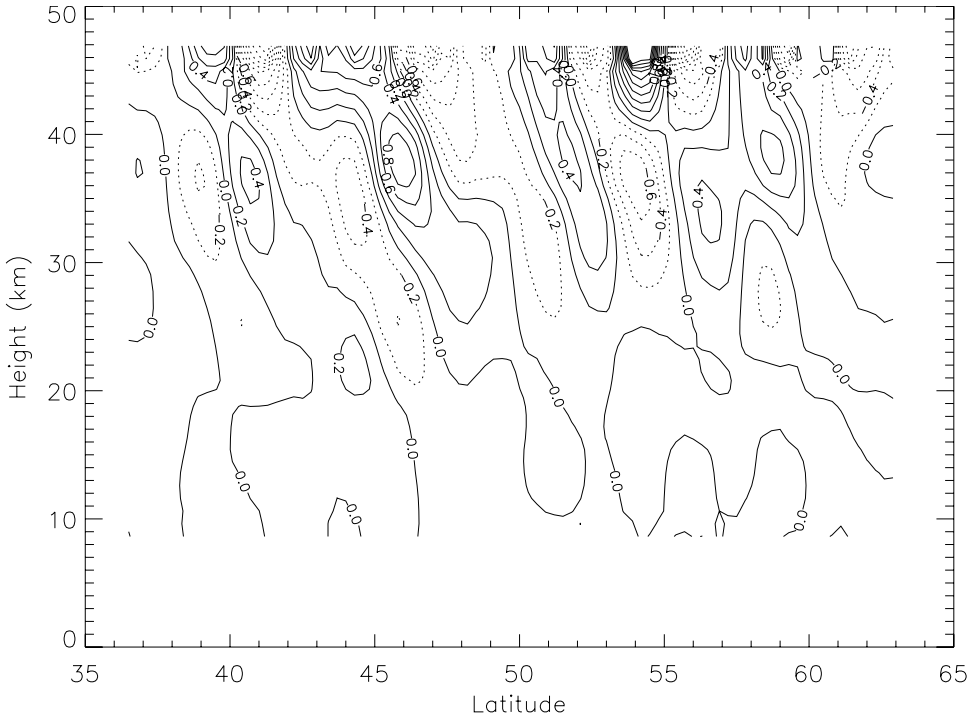

Figure 9. Track and timeline of the wave packet for the first event as seen by channel 13 on 20–21 January 2003. AMSU-A instruments from NOAA 15, NOAA 16, NOAA 17, and NASA Aqua satellites are used to monitor the wave movement in about every 6 hours from the beginning to the end of this transient event.

2003. As shown in Figure 10, the 19–21 January event was the exclusive disturbance over the entire east coast and the NA region in terms of amplitude and duration. The stratospheric wave amplitude is well correlated to the upper tropospheric wave amplitude in the same region (Figure 11). However, the stratospheric responses to the disturbances in the upper troposphere were somewhat selective, as wave propagation depends not only on wave source but also on the background winds.

[27] Unlike the broad and persistent enhancements at 80 hPa the 5-hPa variances show a sharper peak with a shorter duration in region 1 and three transient peaks in region 2, each separated by ~18 hours. The peak in region 1 and the first spike in region 2 are related, corresponding to waves propagating off the east coast with the fast horizontal speed described in Figures 7–9. The first peak in region 2 leads the peak in region 1 in time as expected as the first wave episode propagates from region 2 to region 1. The second and third spikes in region 2 are likely of orographic origin with small horizontal speeds since they did not propagate far enough to reach region 1. They remain in the same region, and the enhanced channel 9 and 13 variances exhibit little time delay, suggesting the fast stratospheric response to disturbances from the troposphere.

3.5. MM5 Simulations

[28] The National Center for Atmospheric Research (NCAR)/PSU nonhydrostatic model MM5 version 3 [*Dudhia*, 1993] is used to investigate the enhanced gravity wave activities observed during 19–21 January 2003 in the east coast of the United States and the NA region. Several mechanisms are likely responsible for exciting these waves in the upper troposphere, including orographic excitation associated with the Appalachians and jet instability associated with the strong trough. The jet was also coupled to precipitation and convective activity in the lower and middle troposphere, which requires model sensitivity studies dedicated to each variable. Only qualitative comparisons of the model simulation to the AMSU-A observations are presented in this paper, whereas more in-depth analyses and sensitivity studies on the dynamics and impacts of these gravity waves are under way and will be detailed in a follow-on paper.

[29] MM5 has demonstrated its capability to simulate realistic wave phenomena associated with baroclinic jet front systems in previous studies [e.g., *Zhang et al.*, 2001]. For this study, the MM5 model domain employs 300 × 200 grid points with 30-km horizontal grid spacing and 90 vertical layers equally spaced from the surface up to 10 hPa, covering the entire North America and NA regions. The European Centre for Medium-Range Weather Forecasts (ECMWF) analysis (archived at NCAR on a 2.5° × 2.5° grid) is used to provide the initial and boundary conditions for the simulations. The MM5 is initialized at 0000 UT on 19 January 2003 and integrated for 36 hours. The medium-range forecast planetary boundary layer scheme [*Hong and Pan*, 1996], Grell cumulus parameterization scheme [*Grell*, 1993], and Reisner microphysics scheme [*Reisner et al.*, 1998] are used in this event simulation.

[30] The MM5 simulation is verified well at large scales against the ECMWF analysis throughout the 36-hour model integration (not shown). In particular, they both simulated well the strength and location of the upper tropospheric jet streak. Inertia GWs are found in the MM5 simulation in the

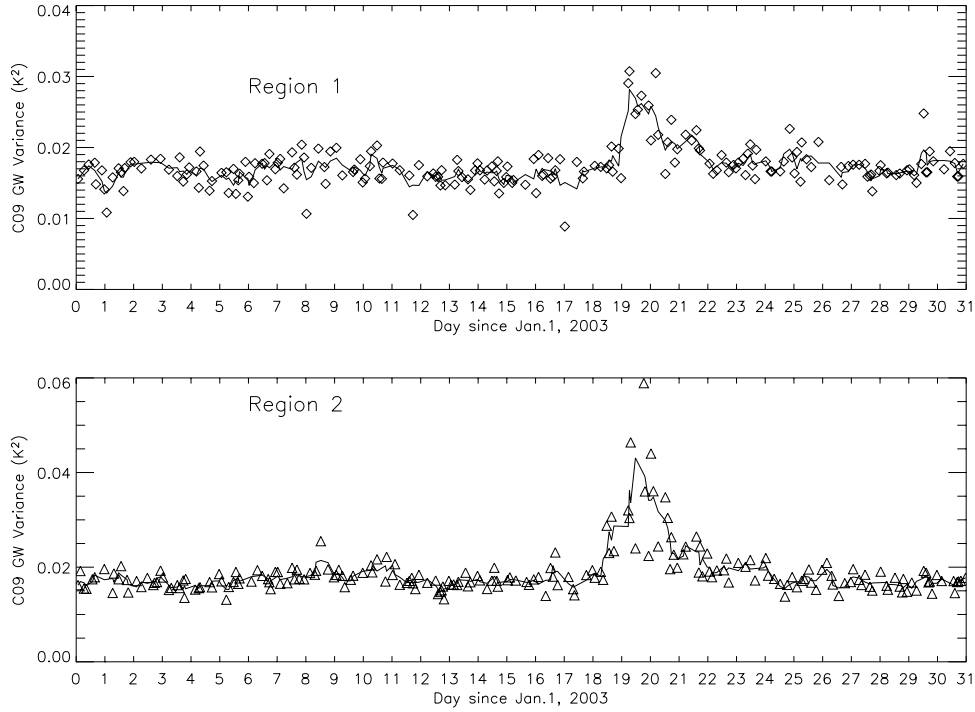

Figure 10. Time series of AMSU-A channel 9 radiance variances for regions 1 and 2 in January 2003. Data from four AMSU-A instruments have been used to produce the time series and have been averaged into hourly bins. Data with the number of samples <100 per bin are excluded in these plots. Noise floor is $\sim$0.02 K^2, and the solid line is the three-point running smooth of the data.

divergence maps (e.g., alternating bands of convergence and divergence) as well as in wind and temperature fluctuations throughout the troposphere and stratosphere. Figure 12 shows that MM5 simulated 80-hPa horizontal divergence overlaid with upper tropospheric (300 hPa) jet streak, which is valid at 1800 UT on 19 January 2003. GW activity is pronounced in several regions, including the Rockies on the far right edge of the polar jet, the Appalachians right ahead

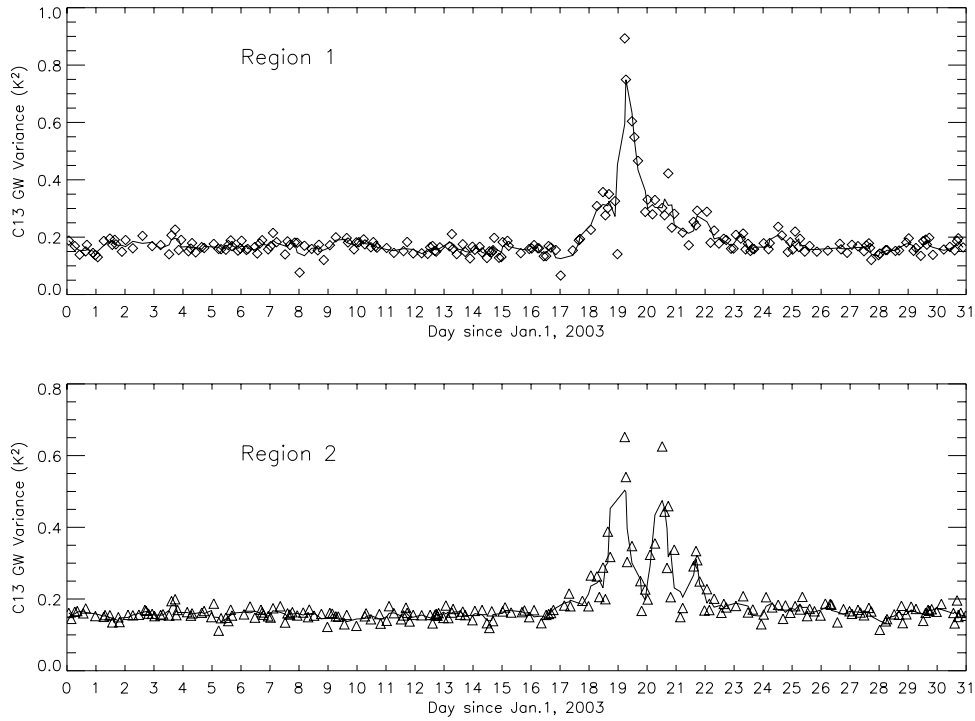

Figure 11. Similar to Figure 10 except for channel 13. Noise floor in this case is $\sim$0.2 K^2.

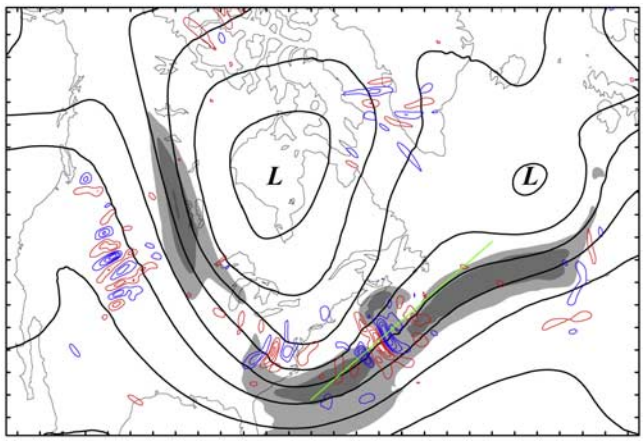

Figure 12. The 80-hPa horizontal divergence (every 3 × 10^{-5} s^{-1}; blue, positive; red, negative), the 300-hPa geopotential heights (every 20 dam), and horizontal wind speed (shaded) from the MM5 simulations at 1800 UT on 19 January (starting on 19 January at 0000 UT). MM5 simulation predicts the two types of GWs seen in AMSU-A channel 9 radiances: one related to jet instability or frontal convection and the other related to the Appalachians. Green straight line indicates where the cross section for Figure 13 is cut.

of the polar jet and behind the subtropical jet, and the North Atlantic slightly to the cyclonic side of the exit region of the main subtropical jet. These GWs are in qualitative agreement with the AMSU-A observations despite a slight eastward shift in location for the NA wave packets.

[31] This flow configuration over the NA and near the east coast of the United States is conducive to GW generation, as shown by *Uccellini and Koch* [1987] and *Zhang* [2004]. As indicated in the AMSU-A observations, these GWs are propagating east and northeastward relative to the ground. The maximum amplitudes of the wind and temperature perturbations found in the simulation are 10 m s^{-1} and 5 K, respectively. The horizontal wavelengths of these waves are approximately 300–400 km. Figure 13 displays a vertical cross section at the same time through the center of the wave packets and along the direction of wave propagation just offshore of the Atlantic coast of the United States. The vertical wavelength shown in Figure 13 is ~8–10 km in the upper troposphere, which is somewhat shorter than the AMSU-A estimate in the upper stratosphere.

[32] In the MM5 simulation, mountain waves over the Appalachians exhibit the dominant horizontal wavelength of ~250 km and vertical wavelengths of >10 km (Figure 13). These waves are transient, as shown in the satellite data, and localized within one to two wavelengths from the mountain source. The waves are mostly amplified on the lee side and tilted toward the upstream. Unfortunately, the vertical extent of the current MM5 simulation is not high enough to determine the fate of these mountain waves and to assess their impact on the upper air dynamics.

4. Discussion and Summary

[33] We studied GW climatology and variability over the U.S. east coast and the North Atlantic region with MLS and AMSU-A radiance measurements during the December–January period. The multiyear AMSU-A observations re-

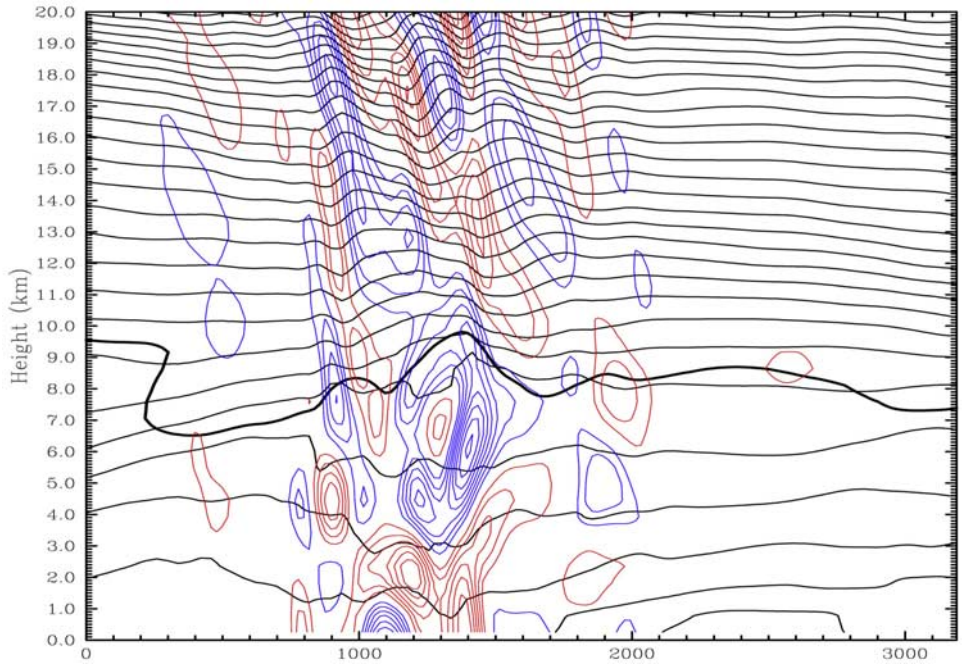

Figure 13. Vertical cross section of horizontal divergence (every 3 × 10^{-5} s^{-1}; blue, positive; red, negative) and potential temperature (black curves, every 8 K) of GWs on January 19 at 1800 UT, cutting through the wave fronts in Figure 12. Tilted wave structure is evident in the troposphere and lower stratosphere. Horizontal wavelengths of these waves vary between 300 and 500 km, whereas vertical wavelengths are seen between 7 and 15 km. Dark thick curve denotes the dynamic tropopause where potential vorticity equals 1.5 potential vorticity units.

veal significant wave activity in this region with strong enhancements in the 1999–2000 and 2002–2003 winters. A detailed analysis was conducted to study the wave properties during a series of episodes on 19–21 January 2003. At least two types of wave excitation were associated with these events: one from cross-Appalachians wind flow and one from baroclinic jet front systems. Typical horizontal wavelengths of 300–600 km and vertical wavelengths of 20–30 km are observed for the waves propagating offshore from the east coast of the United States. Besides the geographical modulation above regions of significant topography the observed GWs in the stratosphere correlate well with intensity and location of the tropospheric baroclinic jet front systems. Furthermore, AMSU-A data show that these wave episodes are transient, normally lasting for 1–2 days, and can reach the upper stratosphere and higher to cause strong mesoscale disturbances in the mesosphere.

[34] A state-of-the-art mesoscale model is used to explicitly simulate the enhanced GW activities identified from satellite observations during 19–21 January 2003. The simulated GWs compared qualitatively well with the satellite observations in terms of wave structures, timing, and overall morphology. Excitation of these large-amplitude mesoscale waves is complicated and requires further dedicated model sensitivity studies and high-resolution observation verifications like those from AMSU-A. Multiple mechanisms have been offered to explain these wave occurrences. The primary mechanisms include geostrophic adjustment [e.g., *Zhang et al.*, 2001; *Zhang*, 2004], shearing instability [e.g., *Einaudi et al.*, 1987], frontogenesis and frontal collapse [e.g., *Snyder et al.*, 1993], and convection [e.g., *Powers and Reed*, 2001; *Lane et al.*, 2001].

[35] More detailed model sensitivity studies are planned to investigate wave generation mechanisms during 19–21 January 2003. Several source mechanisms can often coexist in the region of interest, including (1) topographically forced waves due to jet streaks interrupted by large terrains, (2) adjustment-forced waves due to strong flow imbalance associated with the upper tropospheric jet streaks, (3) diabatically forced waves due to moist convection induced by baroclinic waves, and (4) frontally forced waves due to frontal collapse near the surface. The last three mechanisms are transient in nature and are often inseparable from each other. These mechanisms are currently being investigated with explicit high-resolution mesoscale simulations and advanced diagnostics, which will be reported elsewhere. Moreover, impacts of these large-amplitude waves on the upper atmospheric dynamics and their interactions with larger-scale waves also warrant further investigations.

[36] **Acknowledgments.** Part of this work was performed at the Jet Propulsion Laboratory (JPL), California Institute of Technology, under a contract with the National Aeronautics and Space Administration (NASA), and was funded through the JPL internal Research and Technology Development program. We would like to acknowledge the support from NASA ACMAP program (D.L.W.) and NSF grant ATM-0203238 (F.Z.). We also thank two anonymous reviewers for helpful comments and the NOAA Satellite Active Archive center for making the AMSU data available to this research.

References

Bosart, L. F., W. E. Bracken, and A. Seimon (1999), A study of cyclone mesoscale structure with emphasis on a large-amplitude inertia-gravity wave, *Mon. Weather Rev.*, *126*, 1497–1527.

Chun, H.-Y., and J.-J. Baik (2002), An updated parameterization of convectively forced gravity wave drag for use in large-scale models, *J. Atmos. Sci.*, *59*, 1006–1017.

Dörnbrack, A., T. Birner, A. Fix, H. Flentje, A. Meister, H. Schmid, E. V. Browell, and M. J. Mahoney (2002), Evidence for inertia gravity waves forming polar stratospheric clouds over Scandinavia, *J. Geophys. Res.*, *107*(D20), 8287, doi:10.1029/2001JD000452.

Dudhia, J. (1993), A nonhydrostatic version of the Penn State/NCAR mesoscale model: Validation tests and simulation of an Atlantic cyclone and cold front, *Mon. Weather Rev.*, *121*, 1493–1513.

Eckermann, S. D., and P. Preusse (1999), Global measurements of stratospheric mountain waves from space, *Science*, *286*, 1534–1537.

Einaudi, F., W. L. Clark, D. Fua, J. L. Green, and T. E. VanZandt (1987), Gravity waves and convection in Colorado during July 1983, *J. Atmos. Sci.*, *44*, 1534–1553.

Fritts, D. C., and M. J. Alexander (2003), Gravity wave dynamics and effects in the middle atmosphere, *Rev. Geophys.*, *41*(1), 1003, doi:10.1029/2001RG000106.

Goldberg, M. D., D. S. Crosby, and L. Zhou (2001), The limb adjustment of AMSU-A observations: Methodology and validation, *J. Appl. Meteorol.*, *40*, 70–83.

Grell, G. A. (1993), Prognostic evaluation of assumptions used by cumulus parameterizations, *Mon. Weather Rev.*, *119*, 5–31.

Hamilton, K. (1996), Comprehensive meteorological modeling of the middle atmosphere: A tutorial review, *J. Atmos. Terr. Phys.*, *58*, 1591–1627.

Hong, S.-Y., and H.-L. Pan (1996), Nocturnal boundary layer vertical diffusion in a medium-range forecast model, *Mon. Weather Rev.*, *124*, 2322–2339.

Hoskins, B. J., and K. I. Hodges (2002), New perspectives on the Northern Hemisphere winter storm tracks, *J. Atmos. Sci.*, *59*, 1041–1059.

Jiang, J. H., S. D. Eckermann, D. L. Wu, and J. Ma (2004), A search for mountain waves in MLS stratospheric limb radiances from the winter Northern Hemisphere: Data analysis and global mountain wave modeling, *J. Geophys. Res.*, *109*, D03107, doi:10.1029/2003JD003974.

Kim, Y.-J., S. D. Eckermann, and H.-Y. Chun (2003), An overview of the past, present and future of gravity-wave drag parameterization for numerical climate and weather prediction models, *Atmos. Ocean*, *41*, 65–98.

Koch, S. E., F. Zhang, M. L. Kaplan, Y.-L. Lin, R. Weglarz, and C. M. Trexler (2001), Numerical simulation of a gravity wave event observed during CCOPE. Part 3: Mountain-plain solenoids in the generation of the second wave episode, *Mon. Weather Rev.*, *129*, 909–932.

Koppel, L. L., L. Bosart, and D. Keyser (2000), A 25-yr climatology of large-amplitude hourly surface pressure changes over the conterminous United States, *Mon. Weather Rev.*, *96*, 51–68.

Lane, T. P., M. J. Reeder, and T. L. Clark (2001), Numerical modeling of gravity wave generation by deep tropical convection, *J. Atmos. Sci.*, *58*, 1249–1274.

Lane, T. P., J. D. Doyle, R. Plougonven, M. A. Shapiro, and R. D. Sharman (2004), Observations and numerical simulations of inertia-gravity waves and shearing instabilities in the vicinity of a jet stream, *J. Atmos. Sci.*, in press.

Leutbecher, M., and H. Volkert (2000), The propagation of mountain waves into the stratosphere: Quantitative evaluation of three-dimensional simulations, *J. Atmos. Sci.*, *57*, 3090–3108.

McFarlane, N. A. (1987), The effect of orographically excited gravity-wave drag on the general circulation of the lower stratosphere and troposphere, *J. Atmos. Sci.*, *44*, 1775–1800.

McLandress, C. (1998), On the importance of gravity waves in the middle atmosphere and their parameterization in general circulation models, *J. Atmos. Sol. Terr. Phys.*, *60*, 1357–1383.

McLandress, C., M. J. Alexander, and D. L. Wu (2000), Microwave limb sounder observations of gravity waves in the stratosphere: A climatology and interpretation, *J. Geophys. Res.*, *105*, 1947–1967.

Powers, J. G., and R. J. Reed (2001), Numerical model simulation of the large-amplitude mesoscale gravity-wave event of 15 December 1987 in the central United States, *Mon. Weather Rev.*, *121*, 2285–2308.

Ramamurthy, M. K., R. M. Rauber, B. P. Collins, and N. K. Malhotra (2001), A comparative study of large-amplitude gravity-wave events, *Mon. Weather Rev.*, *121*, 2951–2974.

Reisner, J., R. M. Rasmussen, and R. T. Bruintjes (1998), Explicit forecasting of supercooled liquid water in winter storms using the MM5 mesoscale model, *Q. J. R. Meteorol. Soc., Part B*, *124*, 1071–1107.

Schmidt, J. M., and W. R. Cotton (1990), Interactions between upper and lower tropospheric gravity-waves on squall line structure and maintenance, *J. Atmos. Sci.*, *47*, 1205–1222.

Snyder, C., W. C. Skamarock, and R. Rotunno (1993), Frontal dynamics near and following frontal collapse, *J. Atmos. Sci.*, *50*, 3194–3212.

Uccellini, L. W., and S. E. Koch (1987), The synoptic setting and possible source mechanisms for mesoscale gravity wave events, *Mon. Weather Rev.*, *115*, 721–729.

Wu, D. L. (2004), Mesoscale gravity wave variances from AMSU-A radiances, *Geophys. Res. Lett.*, *31*, L12114, doi:10.1029/2004GL019562.

Wu, D. L., and J. W. Waters (1996), Satellite observations of atmospheric variances: A possible indication of gravity waves, *Geophys. Res. Lett.*, *23*, 3631–3634.

Zhang, D. L., and J. M. Fritsch (1988), Numerical sensitivity experiments of varying model physics on the structure, evolution, and dynamics of 2 mesoscale convective systems, *J. Atmos. Sci.*, *45*, 261–293.

Zhang, F. (2004), Generation of mesoscale gravity waves in the upper-tropospheric jet-front systems, *J. Atmos. Sci.*, *61*, 440–457.

Zhang, F., and S. E. Koch (2000), Numerical simulations of a gravity wave event over CCOPE. Part II: Waves generated by an orographic density current, *Mon. Weather Rev.*, *128*, 2777–2796.

Zhang, F., S. E. Koch, C. A. Davis, and M. L. Kaplan (2001), Wavelet analysis and the governing dynamics of a large amplitude mesoscale gravity wave event along the east coast of the United States, *Q. J. R. Meteorol. Soc.*, *127*, 2209–2245.

Zhang, F., S. E. Koch, and M. L. Kaplan (2003), Numerical simulations of a large-amplitude gravity wave event, *Meteorol. Atmos. Phys.*, *84*, 199–216.

Zhang, F., S. Wang, and R. Plougonven (2004), Uncertainties in using the hodograph method to retrieve gravity wave characteristics from individual soundings, *Geophys. Res. Lett.*, *31*, L11110, doi:10.1029/2004GL019841.

D. L. Wu, Jet Propulsion Laboratory, California Institute of Technology, 4800 Oak Grove Drive, Pasadena, CA 91109, USA. (dwu@mls.jpl.nasa.gov)

F. Zhang, Department of Atmospheric Sciences, Texas A&M University, MS 3150, College Station, TX 77843-3150, USA.